MODELLING OF THE CUTTING PROCESS ANALYTICAL AND SIMULATION METHODS

W. Grzesik, P. Niesłony, M. Bartoszuk

Abstract

The paper presents typical modelling methods of thermal effects in the cutting zone when machining AISI 1045 carbon steel with differently coated carbide tools. The thermophysical properties of the workpiece and tested cutting tool materials were experimentally determined. For multilayer coatings deposited on the carbide tools, the composite layer with equivalent thermophysical properties was applied. Three concepts of modelling of the thermal effects were discriminated, i.e. an analytical algorithm, and FEM and FDM numerical simulations. Selected testing methods were considered in terms of their suitability to evaluate the optimal structures of thermal protective tool coatings and their practical applications.

Keywords: Thermophysical properties, equivalent layer, analytical models, FEM and FDM simulations, coated tools

Modelowanie procesu skrawania – metody analityczne i symulacyjne

Streszczenie

W artykule przedstawiono metody modelowania oddziaływania cieplnego w strefie skrawania stali niskostopowej AISI 1045 narzędziami węglikowymi z naniesionymi różnymi powłokami ochronnymi. Eksperymentalnie wyznaczono właściwości cieplne badanych materiałów obrabianych i narzędziowych. Zaproponowano, do oznaczenia właściwości wielowarstwowych powłok narzędziowych, wykorzystanie idei powłoki kompozytowej o zastępczych właściwościach cieplnych. Przyjęto trzy koncepcje modelowania oddziaływań cieplnych, których podstawą są wyniki obliczeń z użyciem algorytmu analitycznego, oraz symulacji MES i MRS. Wyniki wybranych metod badawczych poddano analizie dla ustalenia ich przydatności w określeniu optymalnej budowy cieplnych powłok ochronnych i ich zastosowania praktycznego.

Słowa kluczowe: właściwości cieplne, powłoka zastępcza, model analityczny, symulacje MES i MRS, narzędzia z powłokami ochronnymi

1. Introduction

In metal cutting operations, temperature rise at the tool-chip interface, and heat transferred from this zone is a crucial factor determining such key process

Address: Prof. W. GRZESIK, P. NIESŁONY, Ph.D. Eng., M. BARTOSZUK, Ph.D., Dept. of Manufacturing Engineering and Production Automation, Opole University of Technology, 45-271 Opole, 5th Mikolajczyka St., Poland, E-mail: w.grzesik@po.opole.pl, p.nieslony@po.opole.pl, m.bartoszuk@po.opole.pl

issues as tool wear and its life, and surface integrity. While heat generation depends mainly on the process parameters and the machinability rate of the work material, the thermophysical properties of the cutting tool material used were found to be a decisive factor in the distribution of temperature fields and heat dissipation rate [1, 2]. In this aspect, the application of tools treated with advanced cutting tool coatings can lead to a substantial reduction of cutting temperatures and increase of the heat partition to the chip and consequently, to moderate tool wear [3, 4]. This is due to the fact that both thermal and tribological outputs from the tool-chip interface are sensitive to changes in the thermophysical properties of the workpiece and coating materials, including thermal conductivity, thermal diffusivity and heat transfer coefficient [5].

There are many analytical and simulation methods which enable determining on average interface temperature or temperature distribution curves along a tool-chip interface [6, 7]. This paper analyzes three different models, one analytical and two numericals, to determine heat flow and temperature distribution in the cutting zone. The range of computated and simulated data obtained with this models is shown in Fig. 1. It should be noted that the analytical model was derived using the new approach to the thermal problems in dry turning of steel with tools coated with multilayer coatings with an intermediate Al_2O_3 layer. In this case, the average of calculated temperatures were compared with the values obtained experimentally by means of the natural thermocouple technique.

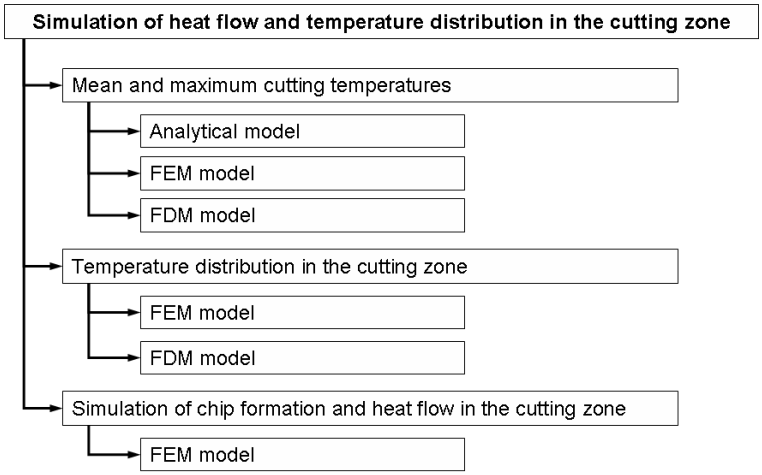

Fig. 1. Range of computed and simulated results obtained with applied models

In order to determine the heat flow and temperature distribution in the cutting zone as well as the chip formation two simulation models based on Finite

Element Method (FEM) and Finite Difference Method (FDM) methods were proposed. Unfortunately, until now, a FDM and few FEM-based simulation techniques (Lagrangian, Eulerian, ALE) are not able to model integrally all physical phenomena involved into complex machining process with engineering accepted accuracy [8]. The thermal or thermodynamical modelling is a bottleneck of FEM and FDM simulations due to uncertainties in arbitrary using such inputs as heat partition coefficient, friction coefficient and both thermal conductivity and diffusivity.

In this paper, three different models were used to model a thermal influences in the cutting zone. The update thermophysical properties of tool and workpiece materials, determined among other input data by means of the advanced Laser Flash and Differential Scanning Calorimeter methods in the Netzsch' research centre, Germany, were implemented into the FEM and FDM models. Additionally, a composite layer, in which all individual layers are replaced by one homogeneous thick layer, was applied to define properties of multilayer coatings [9].

2. Modeling concept

2.1. Determination of models input properties

In the previous research on the modelling of cutting zone using various coated cutting tools, the authors have selected necessary input data to determine analytical and simulation models. In general, the following data should be known:

- mechanical engineering parameters,
- stereometry of tools,
- thermophysical properties of tool and workpiece materials,
- structures of multilayer tool coatings.

2.2. Mechanical engineering parameters and stereometry of tools

In this study, the cutting experiments were conducted using multi-layer coated flat-faced inserts with an intermediate ceramic layer: CVD-TiC/Al_20_3/TiN-Σ10 μm consisting of ISO-P20 cemented carbide substrate. In order to compare the experimental results the substrate was also examined as a reference tool material. The insert geometry was ISO-TNMA 160408 with a clearance angle equal to 0°. The orthogonal cutting tests were carried out on a precision lathe using a thin-walled tube as the workpiece. The cutting was performed dry. The thickness of the tube wall was equal to 2 mm and the outer diameter of the tube was about 80 mm. The work materials used in this study was C45 unalloyed steel equivalent to AISI 1045 carbon steel. During experiments, cutting parameters were selected as follows: the cutting speed

varying from 50 to 210 m/min, constant feed rate f = 0.16 mm/rev and the depth of cut ap = 2 mm.

The measuring techniques were essentially similar to those used in previous author's studies on cutting tool coatings [5, 10, 11]. The cutting F_c and feed F_f forces were measured using a two-component strain-gauge dynamometer fixed on the tool post of a lathe.

The thermal emf signals were recorded in the classical tool-work thermocouple circuit and automatically converted into equivalent temperature values [12]. In the thermocouple experiments, up to 10% variation (sporadically, it was increased to 20% when turning with distinct chatter marks on the machined surface) in the thermoelectric emf measurement was observed in the various sets of test data.

After cutting, the contact parts of the tool rake faces were measured with a PC-based optical image processing system described in [11].

2.3. Thermophysical properties of the tool and workpiece materials

For thermal analysis of the process, the thermophysical properties of workpiece and coating materials occurring at higher temperatures, including thermal conductivity (λ) and thermal diffusivity ($\alpha = \lambda/c_p\rho$), were determined. For example, variations of λ and α with temperature are shown in Fig. 2 [13-15].

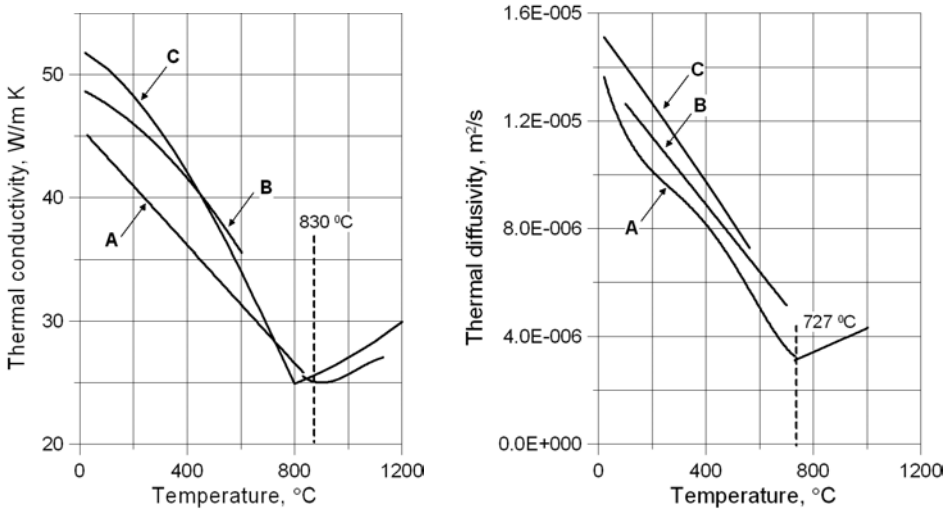

Fig. 2. Dependence of thermal conductivity and diffusivity of AISI 1045 steel on temperature rise. Denotation of symbols: A – own experiment [15], B – [13], C – [14]

Figure 3 presents values of thermal conductivity (3a) and diffusivity (3b) for P20 sintered carbide (WC), TiAlN monolayer and three individual layers involved in TiC/Al_2O_3/TiN multilayer coatings. This data were used to calculate an equivalent thermal conductivity λ_{eq} and diffusivity α_{eq} for a three layer coating based on the composite layer concept (presented as 3L curve in Fig. 3). In this case, for three-layer coatings, the thicknesses of individual layers were assumed to be equal to 6 μm (TiC), 3 μm (Al_2O_3) and 1 μm (TiN). In Fig. 3, symbol 3L-N represents data determined in the Netzsch' research centre – Germany, by means of the Laser Flash and Differential Scanning Calorimeter methods [16].

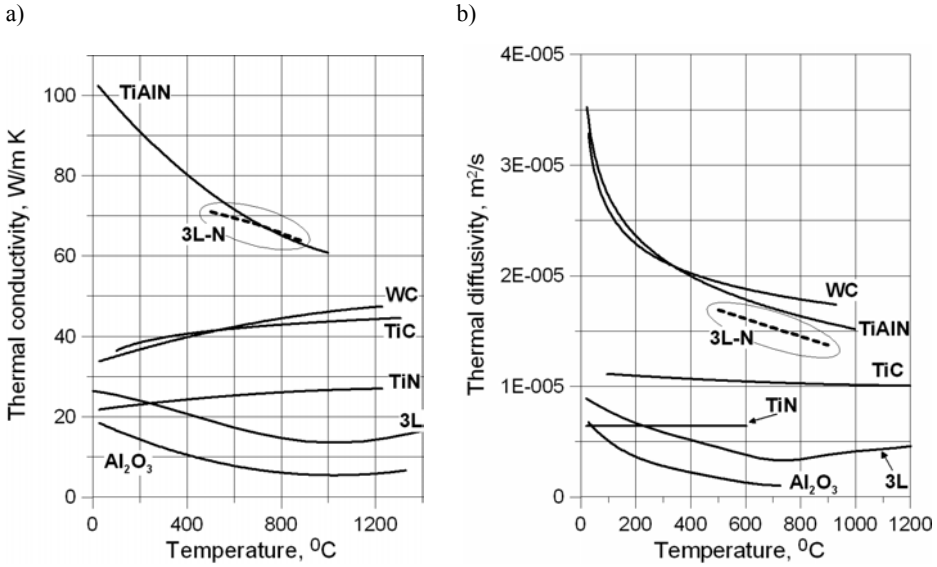

Fig. 3. Thermal conductivity (a) and diffusivity (b) of tool substrate and coating materials vs. temperature

2.4. Composite layer concept

In the composite layer concept, in which all components are replaced by one homogeneous thick layer, the equivalent thermal properties are introduced. Previously, this concept was applied by Balaji and Mohan [17] for prediction of the tool-chip contact and Yen et al. [18] for computer simulation of an orthogonal cutting using the Finite Element Method (FEM).

The equivalent (effective) thermal conductivity for a multilayer structure depends on the thickness of each component and the number of coating layers. The sketch of this idea is presented in Fig. 4. For three layer coating used, it can be determined using well-known thermodynamic formula [13], as follows:

$$\frac{\Sigma x_i}{\lambda_{eq}} = \frac{x_1}{\lambda_1} + \frac{x_2}{\lambda_2} + \frac{x_3}{\lambda_3} \tag{1}$$

where x_i is thickness value of the selected i-layer (i = 1, 2, 3), λ_i is thermal conductivity of i-layer, Σx_i is total thickness of the stack (composite layer), λ_{eq} is the equivalent thermal conductivity of the composite layer.

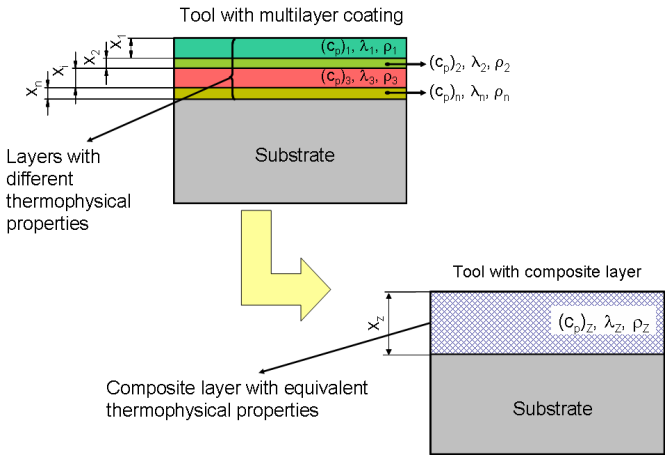

Fig. 4. Diagram of composite layer concept

Analytical and simulations models (FEM and FDM) require values of the thermal diffusivity to be known for actual contact temperatures. It can be determined as the ratio of the equivalent thermal conductivity to the equivalent volumetric heat capacity (C_{eq}). The proper formula can be derived by summing volumes of the individual layers V_i to obtain the total coating. For example, in the case of a three-layer coating it can be written as follows:

$$V = V_1 + V_2 + V_3 \tag{2a}$$

By considering adequate thicknesses (x_i) and densities (ρ_i) of all coating layers and replacing the density by $\rho_i = C_i/c_{pi}$ (where c_{pi} is the specific heat of i-layer) the final equation can be expressed in the form:

$$\frac{\sum_1^t (x_i \rho_i c_{pi})}{C_{eq}} = \frac{x_1 \rho_1 c_{p1}}{C_1} + \frac{x_2 \rho_2 c_{p2}}{C_2} + .. + \frac{x_t \rho_t c_{pt}}{C_t} \tag{2b}$$

where 1 denotes the 1st layer adjacent to the substrate and t identifies the top layer.

Finally, the equivalent thermal diffusivity can be rewritten as:

$$\alpha_{eq} = \frac{\lambda_{eq}}{C_{eq}} \tag{3}$$

2.5. Determination of experimental thermophysical properties of cutting tool materials

The temperature-dependent thermal conductivity $\lambda(T)$ was determined by prior measuring the thermal diffusivity (α) by means of Laser Flesh Apparatus (LFA), specific heat (c_p) by means of a Differential Scanning Calorimeter (DSC), and density (ρ), all as functions of temperature. That is:

$$\lambda(T) = \alpha(T)\rho(T)c_p(T) \tag{4}$$

The accurate description of this experimental methods can be found in previous author's papers, as for example in [16].

3. Physic based modeling of interface temperature

In general, the modelling concept proposed is based on the well-known principle of the simultaneous action of two independent heat sources, which suggests that the total heat flux is generated by aggregation the plastic deformation and sliding friction effects. There is a shear zone (primary deformation zone-PDZ) and frictional heat sources (secondary deformation zone-SDZ). What differenties it from other existing models is that it incorporates actual values of the thermal properties and heat partition coefficients as a function of temperature in one comprehensive model.

In this study, prediction of partition of a heat flux, which flows into a chip, i.e. for body with a moving heat source, was based on the determination of heat partition coefficient (R_{ch}), which defines the percentage of the heat entering the moving chip. It should be noted that fraction ($1 - R_{ch}$) provides the percentage of dissipated energy going to the tool, i.e. the member that is stationary relative to the heat source. For the modelling purpose, three different heat partition coefficients are used [9], namely those proposed by Shaw (R_S), Kato and Fujii (R_{KF}), and Reznikov (R_R).

For calculation of the temperature rise due to plastic deformation in the PDZ three calculation steps were used. In the first one, the thermal number R is

calculated using the Boothroyd's formula [19]. The next two steps of computations are based on the theory of similarity elaborated for metal cutting purpose by Silin [20]. The temperature increment due to the action of the frictional heat source (SDZ) can be determined according to Shaw's [21] or Reznikov [2] formulas.

The computation procedure, presented in Fig. 5, consists of seven subsequent steps for estimating heat partition and interface temperatures. In details, this physic based modelling concept was present in previous author's paper [9].

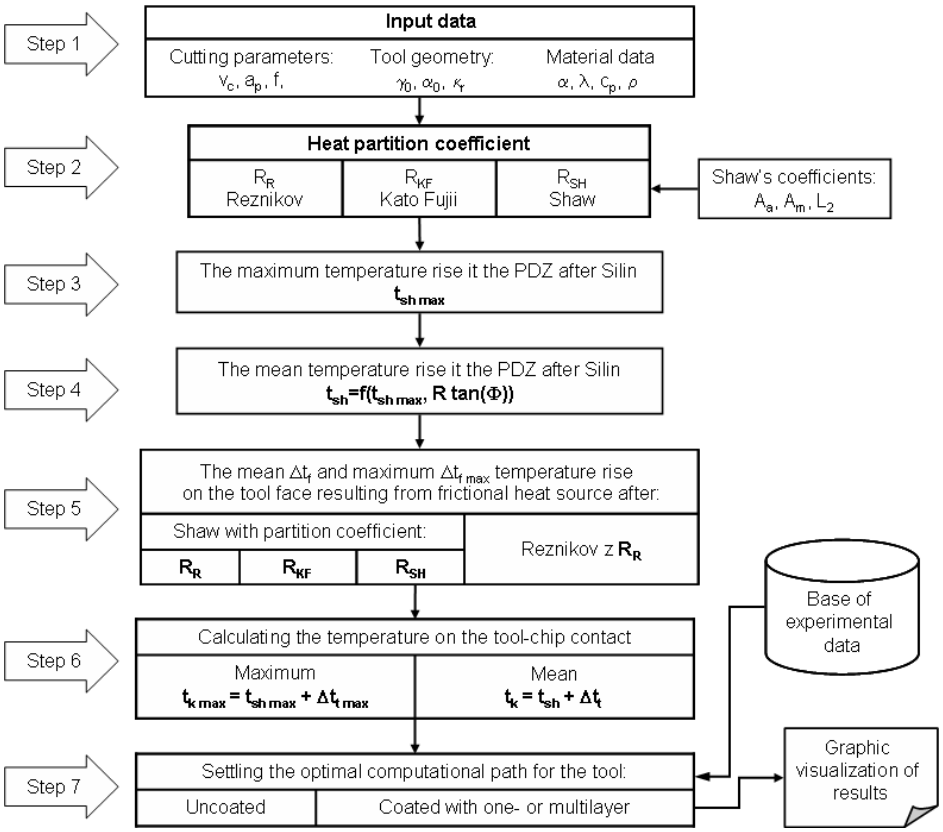

Fig. 5. Flow chart for predicting the peak and average tool-chip interface temperatures

3.1. Computation results and discussion

The analytical methodology developed in section 3 was used to predict the thermal behaviour of the tool-chip interface including the heat partition and the average and peak temperature rise on the rake face of the tested inserts. The

cutting experiments were conducted using one layer coating – CVD-TiAlN-2 μm and one multilayer coating with an intermediate ceramic layer – CVD-TiC/Al_20_3/TiN-Σ10 μm deposited on flat-faced inserts with ISO-P20 cemented carbide substrate. In order to compare the experimental results the substrate was also examined as a reference tool material (P20). The cutting experiment was performed in orthogonal configuration and the measuring techniques were essentially similar to those used in previous author's studies on cutting tool coatings [5, 9, 10]. The work materials used in this study was AISI 1045 carbon steel. During experiments cutting parameters were selected as follows: the cutting speed was varied from 50 to 210 m/min, and constant feed rate f = 0.16 mm/rev, the depth of cut a_p = 2 mm were selected. For the 3-layer coating the equivalent thermophysical properties were used.

The results of computations carried out in this investigation are shown in Fig. 6. The presentation scheme used includes comparisons between measured values of the interface temperatures and the average temperatures calculated (according to the flow chart shown in Fig. 5) for different heat partition coefficient.

It can be observed that the analytical solutions are in good agreement with the thermocouple experiments both in the trend and the absolute values. In case of uncoated and single layer coated tool, good agreement with the measurement data was achieved using Shaw's equation. On the other hand, in case of three-layer coatings with intermediate Al_2O_3 layer, good agreement was obtained using Shaw model and Reznikov partition coefficient. It was documented that these models give good results for tool coated with multilayer coatings with intermediate Al_2O_3 layer [9, 22].

It is possible to predict, with a reasonable accuracy, the average interface temperature based on the equivalent thermal conductivities and diffusivities of the deposited coating materials and the application of the adequate heat partition coefficients. Prediction errors for the average interface temperatures are relatively small in relation to the thermocouple results. They do not exceed 10-15% depending on the type of tool material used. In particular, for the three-layer coatings when cutting speeds ranging from 100-200 m/min, the percentage errors were determined to be not higher than 2%.

4. Finite element modeling of temperature distribution in the cutting zone

Metal cutting is a typical irreversible process, comprising large plastic deformation coupled with temperature rise at high strain rates. From a continuum mechanics point of view, suitable constitutive or governing equations that can describe this phenomenon are needed to predict chip flow, cutting forces, cutting temperature, tool wear, etc. However, the solutions of

displacement or velocity, stress, strain and temperature fields in metal cutting processes have not been easily obtained since large deformations and temperature rise which lead to highly nonlinear and time dependent mechanics of the process.

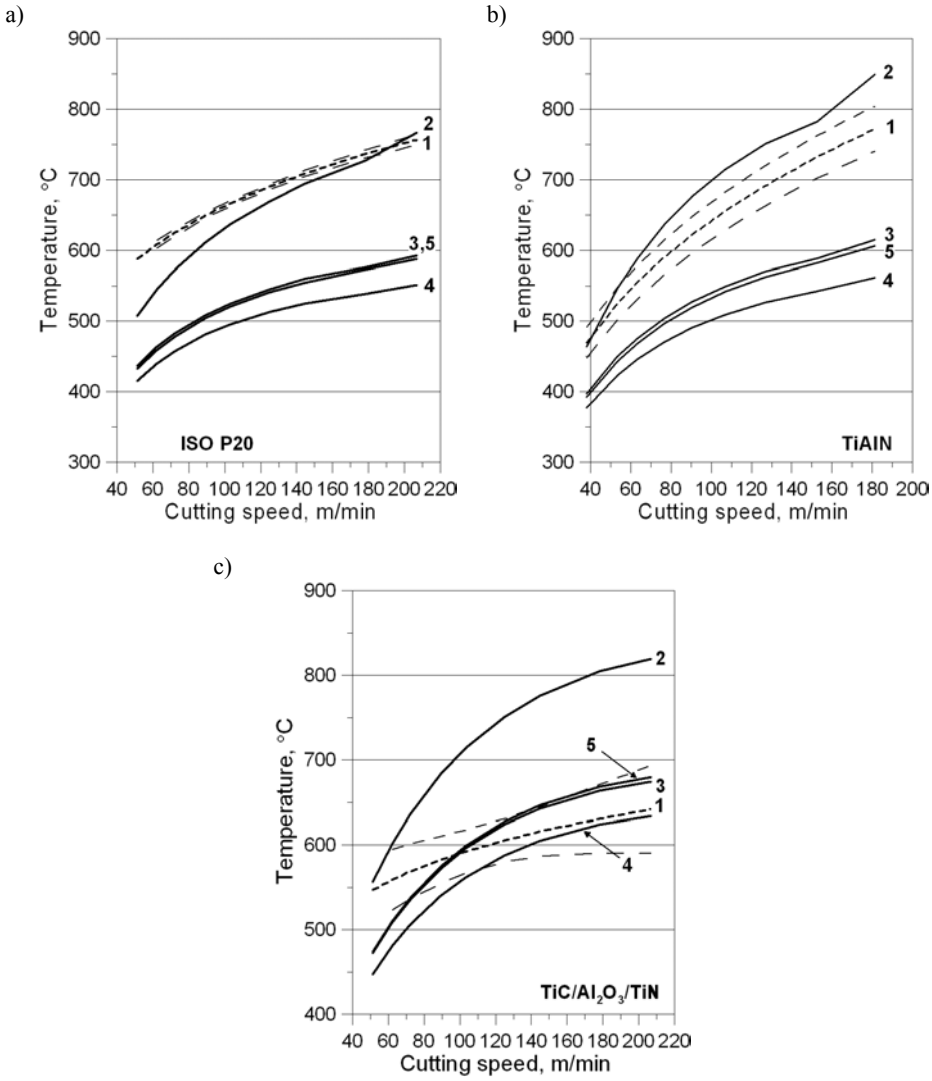

Fig. 6. The average interface temperature vs. cutting speed. Workpiece–AISI 1045 carbon steel: 1 – thermocouple measurements, 2 – after Shaw, 3 – after Shaw and using R_{KF}, 4 – after Shaw and using R_R, 5 – after Reznikov

For the past fifty years metal cutting researchers have developed many modelling techniques including analytical techniques, slip-line solutions, empirical approaches and finite element techniques. In recent years, the finite element method has particularly become the main tool for simulating metal cutting processes [23, 24]. In consequence, temperatures in the tool, chip and workpiece, as well as cutting forces, plastic deformation (shear angles and chip thickness), chip formation and possibly its breaking can be determined faster than using costly and time consuming experiments. Typical approaches for numerical modelling of metal cutting processes are Lagrangian and Eulerian techniques, as well as a combination of both called an arbitrary Lagrangian–Eulerian formulation (ALE) [22, 25].

In this paper, a Lagrangian finite element code AdvantEdge was applied to construct a coupled thermo-mechanical finite element model of plane-strain orthogonal metal cutting with continuous chip formation produced by plane-faced uncoated and differently coated carbide tools. The entire cutting process is simulated, i.e. from the initial to the steady-state phase.

4.1. Inputs data to the FEM simulation package

The workpiece material of choice, AISI 1045 carbon steel, is modeled as thermo-elastic–plastic, while the flow stress is considered to be a function of strain, strain-rate and temperature to represent better behaviour in the cutting process. The tool materials was modeled using the predefined in AdvantEdge software conditions, and using the updated thermal properties of WC-6%Co substrate, TiAlN layer and multilayer CVD-TiC/Al_2O_3/TiN coating system. Both standard and PL-TD material models available in the FEM software AdvantEdge [26] were used. The PL-TD approach uses generally the standard Power Law constitutive model but the user can vary thermal conductivity and heat capacity as functions of temperature.

In addition, three-layer coating was replaced by a multilayer with separately to each layer thermal properties described in [26]. The same goes for a one layer TiAlN. Moreover, the second option was examined by providing the values of thermal properties of the homogeneous 3L layer with equivalent thermal properties (Fig. 3) and for the substrate – TiAlN coating system measured by means of the LF and DSC Netzsch's apparatus (see Section 2.3).

Another inputs were values of the friction coefficient obtained experimentally for the selected cutting speeds range (50-330 m/min) and feed rate of 0.16 mm/rev. It tends to be close to 0.5 at v_c = 330 m/min. The average density of the cutting tool material (substrate plus coating) was assumed to be equal to 1379.4 kg/m^3.

5. Experimental results of fem simulation and discussion

5.1. Cutting temperature

Comparison of the predicted and measured values of the average tool-chip temperatures for the selected tool materials vs. cutting speed is shown in Fig. 7. In general, the "standard" simulation provides substantially higher temperatures in comparison with thermocouple-based measurements. Better agreement was achieved for the PL-TD option and in case of multilayer coated tools for higher speeds, i.e. 200-330 m/min. In this case the equivalent thermal properties for 3L coating were used. On the other hand, for the thin TiAlN layer (Fig. 7c) the Netzsch's data predicted temperatures which underestimate distinctly the measurements (differences are even higher than 50%) in contradistinction to AdvantEdge data (Standard model), where predicted reappraised temperatures in the some order. This discrepancy suggests that microscopic approach to the substrate-coating system does not improve the simulation efficiency. Probably, the most problem in this case is the layer thickness, which is not larger then 2-3 microns.

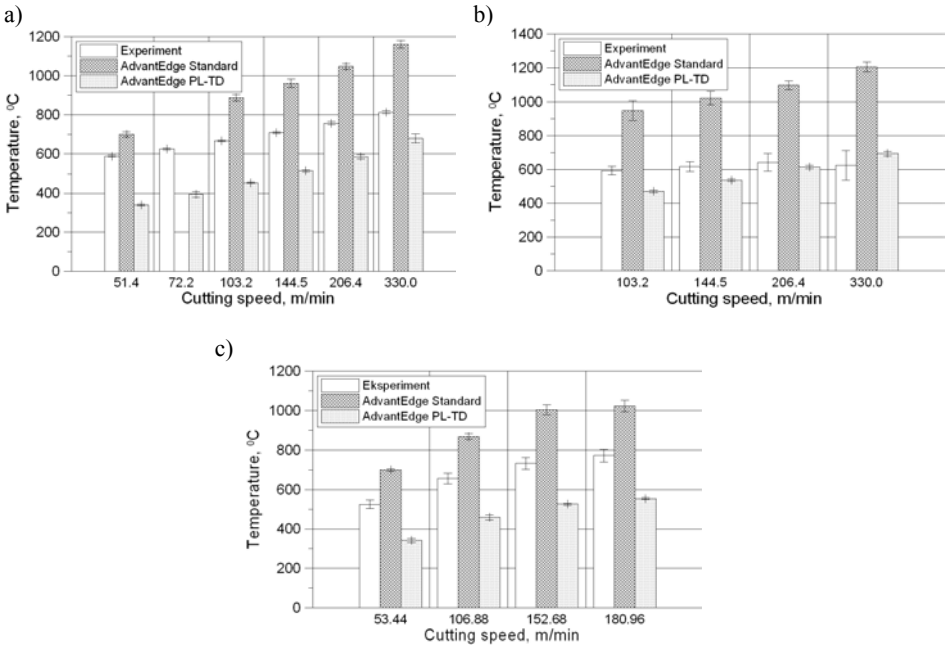

Fig. 7. Comparison of the measured cutting temperatures with FEM simulated values. Tool material: a) ISO P20 carbide, b) 3L coating, c) TiAlN coating. Confidence interval P = 95%

5.2. Distribution of temperature and stresses along the tool-chip interface

The temperature distribution along the tool-chip interface predicted for different simulation conditions and for uncoated and 3L coated tools, is shown in Fig. 8. It is evident from Figs. 8a and 8c that the standard FEM simulation generates temperature distribution curves with distinct peaks, which are localized at a constant distance from the cutting edge. The distance depends on the tool material (0.22 mm for P20 and 0.15 mm for 3L coated P20 carbide). For the PL-TD option a small plateau in the vicinity area of cutting edge is a characteristic feature of these distributions (Fig. 8b,d). It should also be noticed that shorter distance from the cutting edge to the point with temperature stabilization was observed for coated tools.

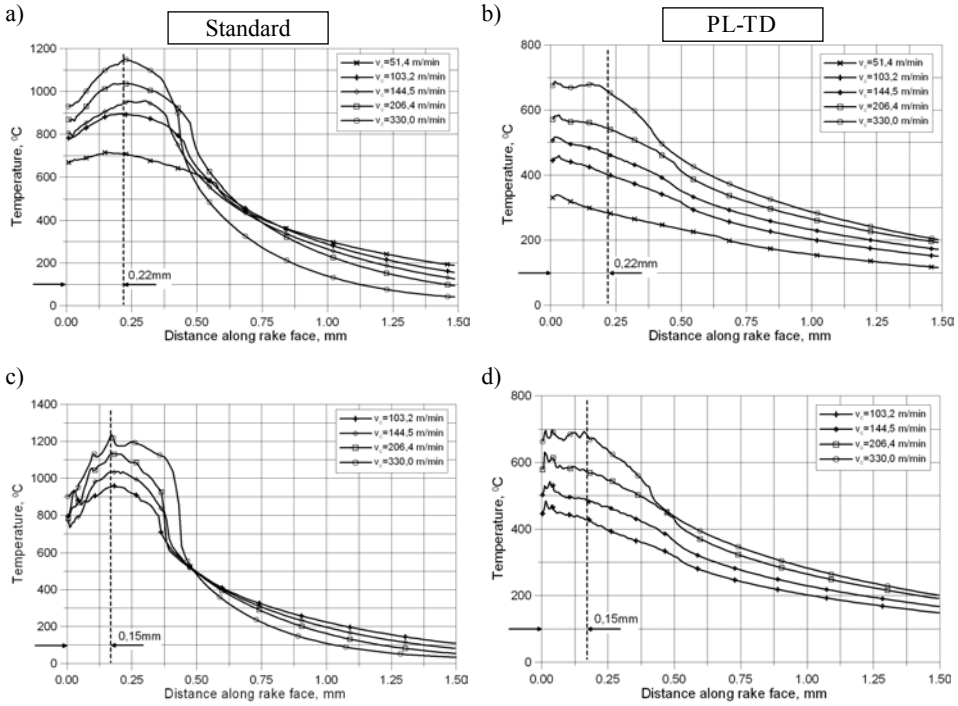

Fig. 8. Temperature distribution along rake face vs. cutting speed for FEM standard and PL-TD simulation: a), b) – P20 uncoated tool, c), d) 3L coated tool

The reduced von Mises stress distributions along the tool-chip interface for different simulation conditions are shown in Fig. 9. The zone Ia can be referred to the seizure region with intensive adhesive interaction. In addition, the boundary between the first (I) and second (II) zones coincides with the points of

maximum interface temperatures. It can be observed that for PL-TD simulation the reduced stress distribution is comparable to model proposed by Lee [27], especially for 3L coated tool and unlike to standard FEM and Zorev [28] stress model.

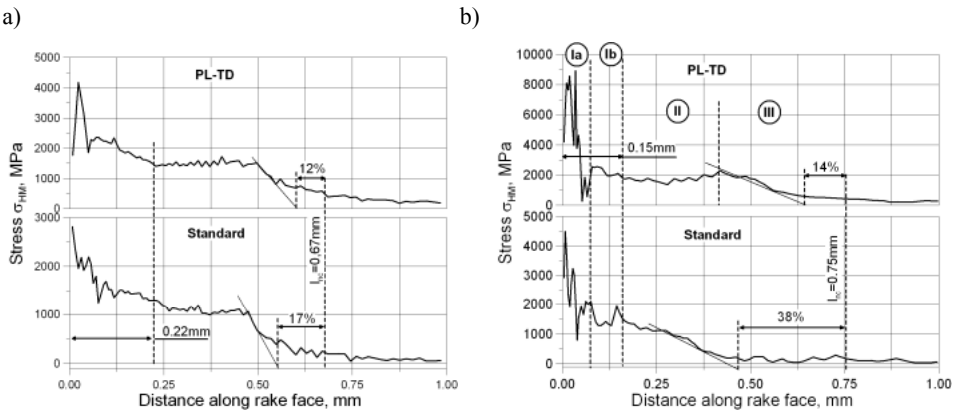

Fig. 9. Distribution of the reduced von Mises stresses along rake face for P20 (a) and 3L coated tools (b) (v_c = 103.2 m/min)

5.3. Visualization of thermal behaviour of the cutting zone

Some characteristic temperature maps covering the primary and secondary deformation areas obtained for different thermophysical data are shown in Fig. 10. In case of the PL-TD variant (Fig. 10b) the chip is visibly thicker and the field of higher temperatures is more extended in the chip. On the other hand, the maximum temperature, for the 3L coating, of about 700^0C is localized closer to the cutting edge and the tool contact area is cooler (about 550^0C). For example, the relevant temperatures recorded for "standard" simulation (Fig. 10a) are equal to 1020^0C and 950^0C, respectively.

It should be noted that for the PL-TD we obtained better conformity of the chip thickness and contact length apply to the experimental data [22]. This may suggest a better fit of the constitutive tool/coatings material model to simulate the frictional interactions at the tool-chip contact area.

The finite element simulation performed demonstrates the existence and localization of too heat zones. It was observed that simulation option and input thermophysical data of the tool materials are decisive factors in obtaining proper temperature values in both PDZ and SDZ.

For 3L coated tools the best coincidence of experimental and modeled temperatures were obtained for PL-TD option and composite coating which represents "micro" approach to thermal functions of the coating deposited. Temperature distribution patterns have some visible physical analogies to the

reduced von Mises stresses and tool-chip contact behaviour. In particular, it was documented that the FEM simulation options influence the reduced stress distribution along the rake face. In this case too models proposed by Lee (for PL-TD) and Zorev (for standard FEM) were specified.

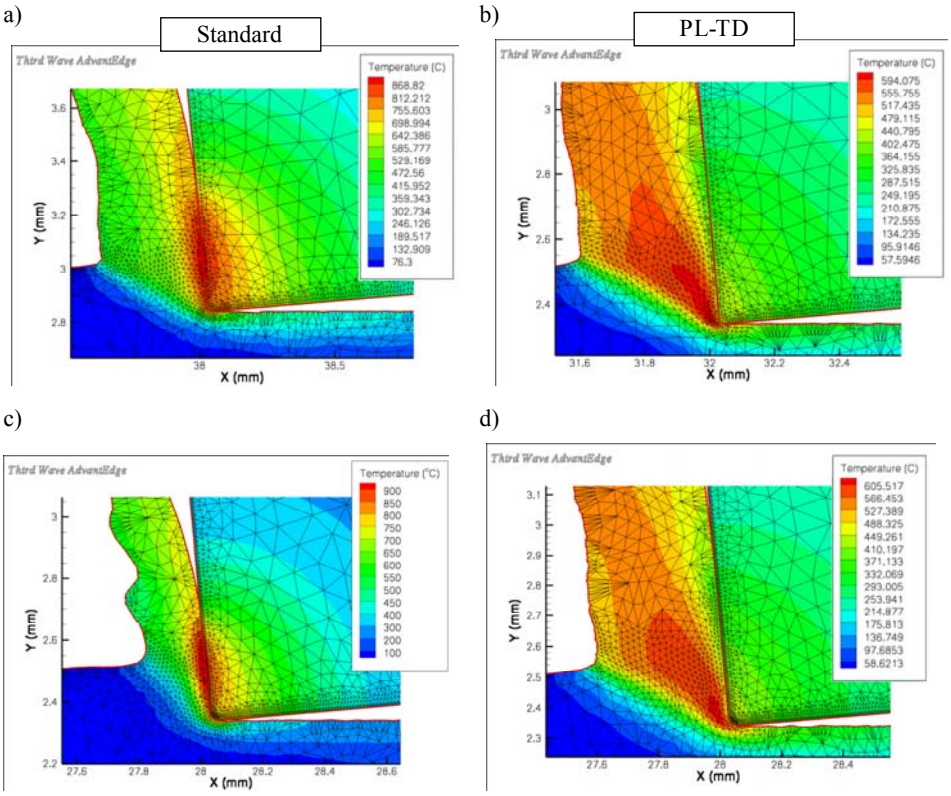

Fig. 10. Thermal maps obtained by FEM standard and PL-TD simulation: a), b) – P20 uncoated tool, c), d) 3L coated tool (vc = 103.2 m/min)

6. Finite difference methods used to modelling temperature distribution in the cutting zone

It is well known that the determination of the tool isotherms and temperature distribution on the rake face have been performed by utilizing experimental, analytical and numerical methods. The usual numerical methods such as the finite element (FEM), the finite difference (FDM) and the boundary element (BEM) methods can be applied to solve the heat transfer problem in metal cutting. FEM and FDM are amongst the common techniques used to study the forward thermal problem in machining. The FEM simulation method

proposed by authors for determination temperature distribution in coated sintered carbon tools was presented in section 5.

The FDM technique was often used for predicting the steady-state tool and chip temperature fields in continuous machining [29-32]. In this case, FDM-based simulation needs some experimental results enabling determination of the average tool-chip interface temperature and heat flux rate resulting from the frictional heat source.

In this paper present FDM simulation results were obtained for two models defined by authors. First, it is a steady-state model which contains only a tool material, and second is non-stationary model which additionally covers the chip material.

6.1. Analytical models of conduction of heat and boundary conditions

Heat flow in an isotropic solid is known in thermodynamics as heat conduction. Its behaviour is obviously described by Fourier's law expressed in the form:

$$\dot{q} = -\lambda \nabla T \tag{5}$$

where: $\dot{q}$ is the heat flow rate, ∇T (in Km^{-1}) is the local temperature gradient (Hamilton's vectoral operator-nabla) and λ is the thermal conductivity.

For the two-dimensional model (the isothermal surface) the temperature T at the point $P(x,y,t)$ will be a continuous function of coordinate axes x and y at time t. Thus, the general conduction equation (Fourier-Kirchhoff equation) in Cartesian coordinates for a steady-state heat conduction can be expressed as [33]:

$$\frac{\partial T}{\partial t} = \alpha \nabla^2 T + \frac{\dot{q}_v}{c_p} \tag{6}$$

where: $a = \lambda/(c_p \rho)$ is the thermal diffusivity of the substance, c_p is specific heat capacity and ρ is the density.

In the case of steady heat flow (steady-state model) for which the derivative $\frac{\partial T}{\partial t} = 0$ and the absence of the net heat flow into the element Equation 6 can be simplified to the Laplace's formula as:

$$\frac{\partial^2 T(x,y)}{\partial x^2} + \frac{\partial^2 T(x,y)}{\partial y^2} = 0 \tag{7}$$

On the other hand, the non-stationary model can be defined using a Fourier equation. For the some conditions as in the first case, this formula can be written as:

$$\frac{\partial T(x,y,t)}{\partial t} = \alpha \left(\frac{\partial^2 T(x,y,t)}{\partial x^2} + \frac{\partial^2 T(x,y,t)}{\partial y^2} \right) \tag{8}$$

The graphical presentation of boundary conditions used for determination of the both FDM models is illustrated in Fig. 11.

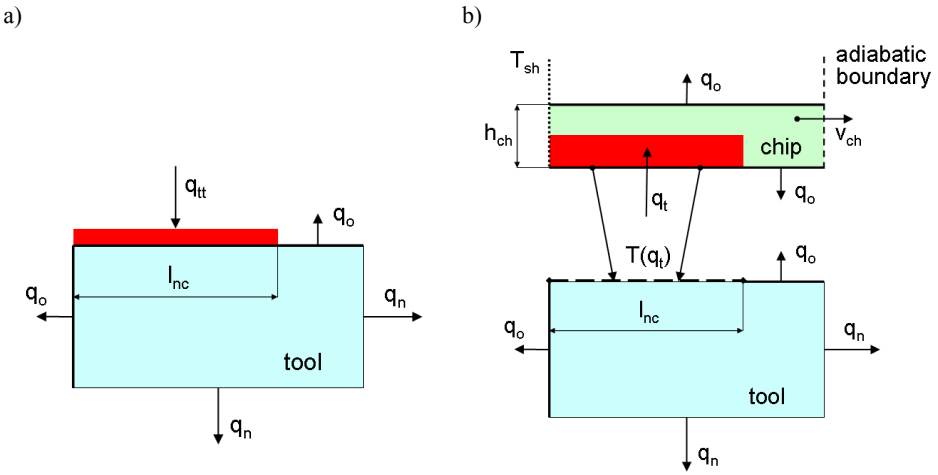

Fig. 11. Boundary conditions for the temperature field in the cutting zone for steady-state (a) and non-stationary (b) FDM heat transfer models

In the case of first steady model, the input properties enclose heat conduction to surroundings air q_0, heat conduction to the tool q_n, and heat conduction into tool q_{tt} along the tool-chip contact length l_{nc}. This parameter was calculated using analytically determined partition coefficient of heat generated in SDZ (see section 3). In particular, the non-stationary model uses partially the same boundary conditions. Additionally, the heat conduction q_t in the SDZ was defined (by analytical method). Based on these data temperature at tool-chip contact zone $T(q_t)$, the chip thickness h_{ch}, and its speed v_{ch} were calculated. Using an analytical algorithm and experimental data the mean temperature on the shear plane T_{sh}. was calculated.

The calculation method applied by authors for solving difference equations is a special variant of the FDM called the method of elementary balances (MBE) in which difference equations are defined based on balances of energy for all discrete elements of the model. The calculation methodology, computation algorithm and all formulas can be found in previous author's papers, as for example in Refs. [34-36].

6.2. Experimental results of simulation for the steady-state FDM heat transfer model

In particular, the simulated temperatures were computed by numerical integration of the temperature distribution at the tool-chip interface as the arithmetic averages. In order to explain the possible sources of discrepancies between the results compared, real variations of the measured temperatures are also marked on the appropriate bars. It can be seen in Fig. 12 that the FDM simulation provides higher mean average temperatures (bars #2) along the tool-chip interface than the multilayer $TiC/Al_2O_3/TiN$ coatings used.

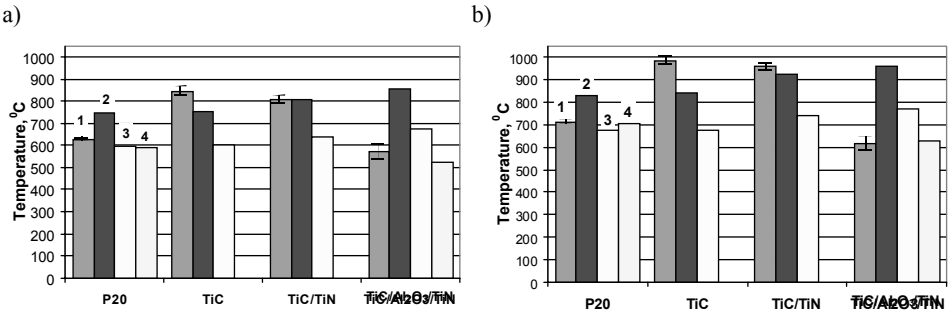

Fig. 12. Comparison of predicted and measured tool-chip interface temperatures for different cutting speeds: (a) 72m/min, (b) 145m/min; 1 – measurement, 2 – arithmetic average, 3 – numerical integration, 4 – analytical modelling [9]

It is interesting to note that analytical models proposed recently by authors in Ref. [9] allow obtaining the average temperatures (bars #4) for uncoated and three-layer coated tools, comparable to the results of FDM simulation performed. As shown in Fig. 12b, the predictions for these above-mentioned tools fit very well for P20-C45 pair (705 and 670^0C) and pretty well for P20-$TiC/Al_2O_3/TiN$ pair (626.5 and 770^0C).

Taking into account relatively high scatter of the emf signals for a $TiC/Al_2O_3/TiN$ coating, it is concluded that the proposed model predicts 1-20% lower or higher temperature values compared with experimental results. Moreover, the accuracy depends on the value of the computed average interface temperature selected. On the other hand, the accuracy of temperature prediction depends on the number of iterations, as shown in Fig.13. If the number

of iterations increases from 7500 to 12500, the average temperature rises from 650 to 780 ^{0}C, as shown on the bar inside Fig. 13.

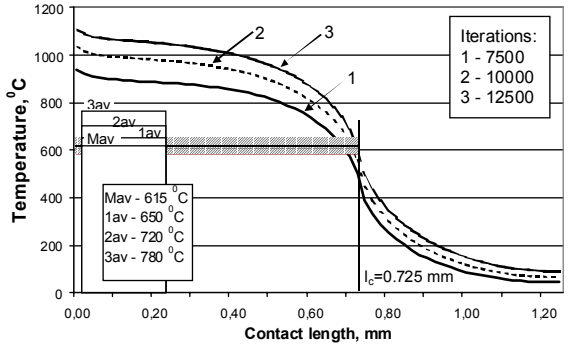

Fig. 13. Influence of iteration number on the predicted temperature distribution. Coating–TiC/Al_2O_3/TiN, cutting speed = 145m/min

The temperature distributions along the tool-chip interface for uncoated and 3L coated tools and different cutting speeds are depicted in Fig. 14. As can be observed from the temperature distribution curves, the increase of the cutting speed from 72 to 145 m/min causes the maximum temperature rises from 810 to 910^{0}C for uncoated P20 carbide, and from 970 to 1095^{0}C for ceramic based TiC/Al_2O_3/TiN coating. Presumably, the higher contact temperature of 1095^{0}C revealed for three-layer coating depend on the thermal conductivity of tool materials, especially on Al_2O_3 intermediate layer used.

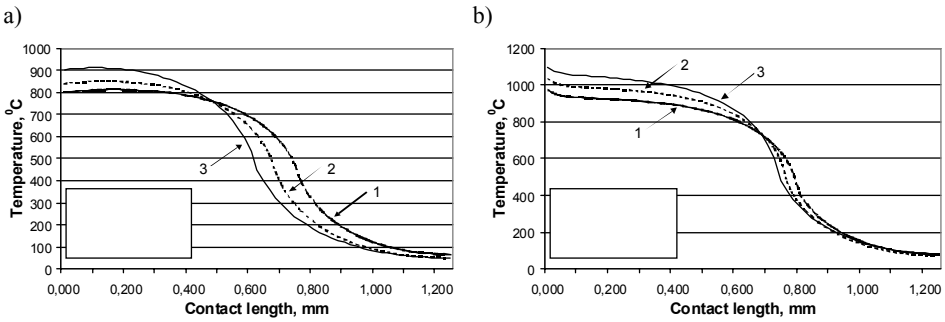

Fig. 14. Influence of cutting speed on temperature distribution along the tool-chip interface. Cutting tool material: a) P20 carbide, b) TiC/Al_2O_3/TiN coated carbide

The discrepancies between calculated and measured values of tool temperatures can lay in the heat flux reflection from the cutting tool tip surfaces, temperature dependence of the thermal properties of tool material and workpiece

temperature rise. Surprisingly, it was proven that the heat flux distribution iterated only small changes in the temperature field. In contrast, it is suggested [37] that the shape of heat source influences the location of the maximum interface temperature, but it remains the same value.

For this reason, the authors suggested to carrying out simulations tests with various heat source shapes presented in Fig. 15.

Heat source shape	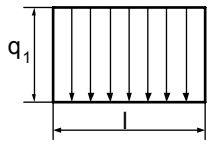 Version I (uniform)	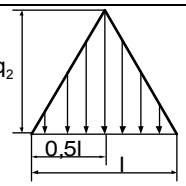 Version II (triangle)	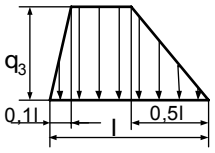 Version III (trapez)
Max. value of q	q_1	$q_2=2q_1$	$q_3=1,43q_1$

Fig. 15. Shapes of heat source used in the FD simulations

The distribution of tool-chip interface temperatures determined for all shapes of heat source, along with the measured average temperature, are integrally presented in Fig. 16.

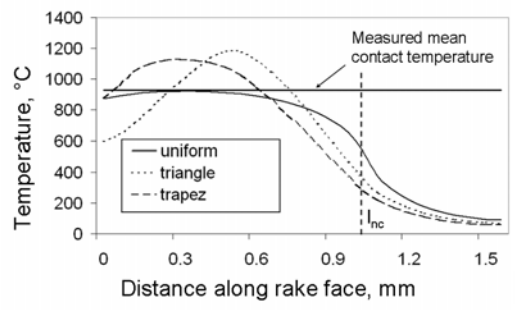

Fig. 16. Distribution of temperature at the tool-chip interface for different heat source shapes and cutting speed v_c = 160 m/min. Conditions: tool-P20 carbide, workpiece-AISI304 stainless steel

It is evident that the shape of heat source influences both the peak temperature and its location at the interface. Particularly, triangular heat source can develop peak temperature of 170^0C, higher than for commonly used plane heat distribution. Authors suggest [36] that the simulation accuracy depends not only on the model formulation, including both initiating and boundary conditions but primarily on the shape of heat source. In particular, acceptable

agreement between computed and measured values of the average interface temperatures was obtained for trapezoidal shape of the heat source, similar to the distribution of contact shear stresses.

6.3. Experimental results of simulation for the non-stationary FDM heat transfer model

Modeling of heat distribution in the cutting zone can be developed using RS models, which allow to create a simulation model for the non-stationary heat transfer. In this case the composed FDM model is based on the Fourier equation (8). The changes of heat flux values are dependent on time. Nieslony proposed [22], to timing the completion of the iterative calculation process using a criterion equation. The criterion of calculation termination of the differentiable heat conduction equation was defined as:

$$\Delta T_{iter} = \frac{\overline{T}_{k(i)} - \overline{T}_{k(i-n)}}{i-(i-n)} \quad {}^{o}\text{C/iteration} \tag{9}$$

where T_k is mean contact temperature, i is iteration number and n is following number.

Authors assess this quantity on the level of $\Delta T_{iter} \leq 0.002$ ^{o}C/iteration.

Figure 17 presents the influence of iteration number on the mean contact temperature for different cutting speeds. It can be seen in Fig. 17 that for the greater number of iteration (time) the average contact temperature achieves almost constant value. The end of iteration, resulting from the criterion ΔT_{iter}, is strictly bounded with cutting speed. For the higher speed, the iteration number is about 10000-15000, where for the lower number is about 17000 iterations more.

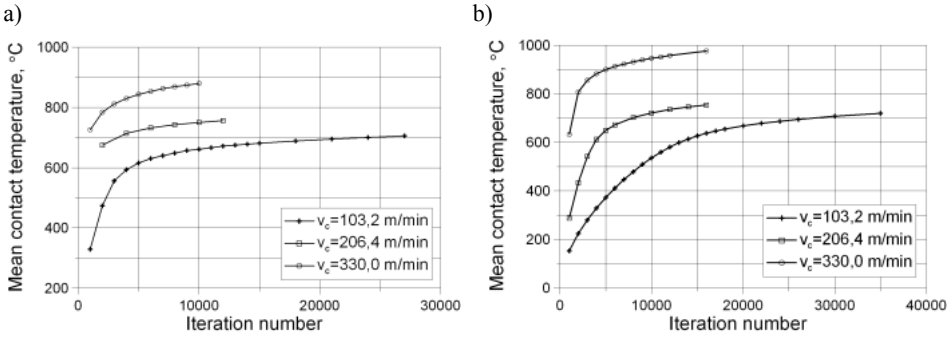

Fig. 17. Influence of iteration number on mean contact temperature for different cutting speeds when machining AISI 1045 steel with P20 carbide tool (a) and 3L coated tool (b)

The differences in computed and measured temperature are compared, for the two couple AISI 1045 steel – uncoated and 3L coated tool, in Fig. 18. It can be seen that the FDM simulation provided higher average temperatures in all tested cases, but the measured and computed values are comparable with each other assuming the probability range of variation at P = 95%. This is a better compliance than for the FDM simulation where steady-state heat transfer model (see section 6.2) was used. On the other hand, in this case the total heat flow calculated from experimental data was computed. It was not necessary to calculate the heat partition coefficient and quantify the amount of heat which penetrates to the tool.

The temperature fields simulated by means of the FD method are presented in Fig. 19.

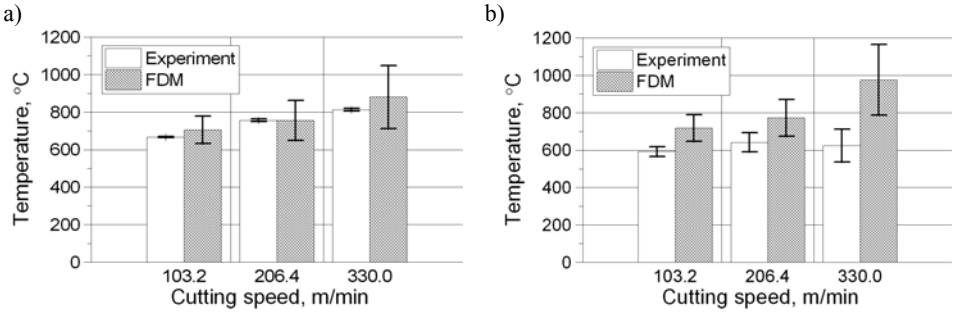

Fig.18. Comparison of predicted and measured tool-chip interface temperature for different cutting speeds by machining AISI1045 steel with P20 carbide tool (a) and 3L coated tool (b) (range of variation for P = 95%)

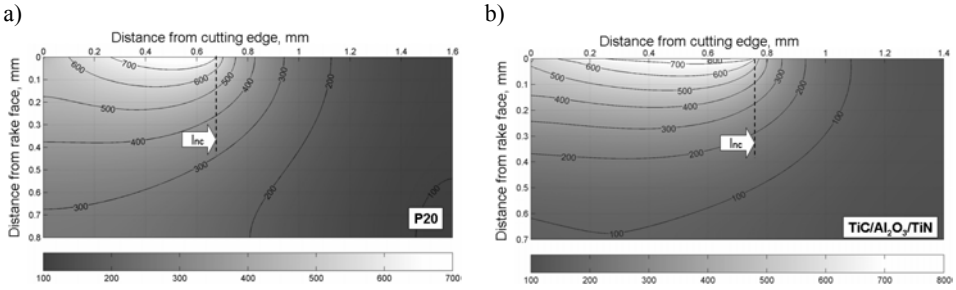

Fig. 19. Temperature fields for a AISI 1045 steel coupled with P20 carbide tool (a) and 3L coated tool (b). Cutting speed = 100 m/min

The first important observation from the temperature distributions obtained for both uncoated and coated tools and the cutting condition used is that the maximum temperature fields are localized near the end of rake face – chip l_{nc}

contact. It should be noted that the uniform shapes of heat source was used. The tests with another shapes of heat source (not published data) confirm a large influences of these factor. The modification of the heat source shape is a good way to optimization of the process simulations for a range of thermal influences.

7. Conclusions

Modelling of coated tool materials requires the proper determination of thermophysical properties using experimental or analytical methods including composite (equivalent) layer concept.

Analytical model allows to predict the average and maximum values of temperature changes as a function of cutting speed for carbide sintered tools with different tool coatings.

The main condition which enables the optimalization of the calculation algorithm is applying the different heat partition coefficients and providing, the equivalent layer concept for the multilayer coatings

For the FEM modeling, it is important to define the constitutive models of tested workpiece and tool materials.

It was possible, by taking into account the thermo-physical properties of tested materials, to quantify the influence of tool coatings on the performance of cutting process.

It was found that the FDM-based simulation model with non-stationary heat flow allows simple, quick and correct simulation of temperature distribution in the cutting zone.

Moreover, the effect of heat source shapes on temperature distribution in the tool was considered.

Currently, it is not possible to provide one optimal method for analysis of thermal effects in the cutting zone. Methodology proposed by the author's is based on the different methods of modelling, i.e. analytical, FEM and FDM simulations and their experimental validation.

References

[1] E.M.TRENT, P.K. WRIGHT: Metal Cutting. 4th ed., Butterwoth-Heinemann, Boston 2000.

[2] A.N. REZNIKOV: Thermophysical aspects of metal cutting processes (in Russian). Mashinostroenie, Moscow 1981.

[3] W. GRZESIK: Advanced protective coatings for manufacturing and engineering. Hanser Gardner Publications, Cincinnati 2003.

[4] W. KÖNIG, R. FRITSCH, D. KAMMERMEIER: Physically vapour deposited coatings on tools: Performance and wear phenomena. *Surface and Coatings Technology*, **49**(1991), 316-324.

[5] W. GRZESIK, P. NIESLONY: Thermophysical-property-based selection of coatings for dry machining of carbon and stainless steels. *Trans. ASME J. Manufact. Sci. Technol.,* **125**(2003), 689-695.
[6] R. KOMANDURI, Z.B. HOU: Tribology in metal cutting-some thermal issues. *Trans. ASME, Journal of Tribology*, **123**(2001), 799-815.
[7] L. LAZOGLU, Y. ALTINAS: Prediction of tool and chip temperature in continuous metal cutting and milling. *Int. J. Mach. Tools Manufact*., **42**(2002), 1011-1022.
[8] T.H.C. CHILDS, K. MAEKAWA, et al.: Metal cutting. Theory and applications. Arnold, London 2000.
[9] W. GRZESIK, P. NIESŁONY: Physics based modelling of interface temperatures in machining with multilayer coated tools at moderate cutting speeds. *J. of Machine Tools & Manufacture*, **44**(2004), 889-901.
[10] W. GRZESIK, P. NIESLONY: A computational approach to evaluate temperature and heat partition in machining with multilayer coated tools. *J. Mach. Tools Manufact*., **43**(2003), 1311-1317.
[11] W. GRZESIK: The influence of thin hard coatings on frictional behaviour in the orthogonal cutting process. *Tribol. Int*., **33**(2000), 131-140.
[12] W. GRZESIK: Experimental investigation of the cutting temperature when turning with coated cutting inserts. *J. Mach. Tools Manufact*., **39**(1999), 355-369.
[13] Charakterystyka stali. Stale do prac w temperaturach podwyższonych i obniżonych. Seria D, Wydawnictwo „Śląsk", Katowice 1984.
[14] Material Properties Database, MPDB v6.55, JAHM Software, Inc., 2003.
[15] W. GRZESIK: A revised model for predicting surface roughness in turning. *Wear*, **194**(1996), 143-148.
[16] P. NIESLONY: Thermal modelling of the cutting process using fem simulation with updated thermophysical properties of tool materials. *Advances in Manufacturing Science and Technology,* **32**(2008)3, 15-25.
[17] A.K. BALAJI, V.S. MOHAN: An 'effective cutting tool thermal conductivity' based model for tool-chip contact in machining with multi-layer coated cutting tools. *J. Mach. Sci. Technol*., **6**(2002)3, 415-436.
[18] Y.-C. YEN, A. JAIN, P. CHIGURUPATI, W.-T. WU, T. ALTAN: Computer simulation of orthogonal cutting using a tool with multiple coatings, Proc. 6th CIRP Inter. Workshop on Modeling of Machining, Hamilton, Ontario 2003, 1-10.
[19] G. BOOTHROYD, W.A. KNIGHT: Fundametals of machining and machine tools. Marcel Dekker, New York and Basel 1989.
[20] S.S. SILIN: Similarity methods in metal cutting. Mashinostroenie (in Russian), Moscow 1981.
[21] M.C. SHAW: Metal cutting principles. Clarendon Press, Oxford 1989.
[22] P. NIESŁONY: Modelowanie przepływu ciepła i rozkładu temperatury w strefie skrawania dla ostrzy z twardymi powłokami ochronnymi. Oficyna Wydawnicza Politechniki Opolskiej, Opole 2008.
[23] S.M. ATHAVALE, J.S. STRENKOWSKI: Finite element modelling of machining: from proof-of-concept to engineering applications. *Mach. Sci. Technol.,* **2**(1998)2, 317-342.

[24] F. KLOCKE, T. BECK, S. HOPPE, T. KRIEG, et al.: Examples of FEM application in manufacturing technology. *J. Mater. Process. Technol*., **120**(2002) 450-457.
[25] M.R. MOVAHHEDY, M.S. GADALA, Y. ALTINTAS: Simulation of chip formation in orthogonal metal cutting process: an ALE finite element approach. *Mach. Sci. Technol*., **4**(2000)1, 15-42.
[26] Third Wave *AdvantEdge* 2D User's Manual, Version 5.0, Minneapolis 2006, USA.
[27] L.C. LEE, X.D. LIU, K.Y. LAM: Determination of stress distribution on the tool rake face using a composite tool. *J. Mach. Tools Manuf*., **35**(1995)3, 373-382.
[28] N.N. ZOREV: Interrelation between shear processes occurring along tool face on shear plane in metal cutting. *Res. Prod.,* (1963), 42-49.
[29] I. LAZOGLU, Y. ALTINTAS: Prediction of tool and chip temperature in continuous and interrupted machining. *Int. J. Mach. Tools Manufact*., **42**(2002), 1011-1022.
[30] M.A. DAVIES, Q. CAO, A.L. COOKE, R. IVESTER: On the measurement and prediction of temperature fields in machining AISI 1045 steel. *Annals of the CIRP* **52**(2003)1, 77-80.
[31] A.J.R. SMITH, E.J.A. ARMAREGO: Temperature prediction in orthogonal cutting with a Finite Difference Approach. *Annals of the CIRP*, **30**(1981)1, 9-13.
[32] C.B. ALUWIHARE, E.J.A. ARMAREGO, A.J.R. SMITH: A predictive model for temperature distributions in "classical" orthogonal cutting. *Trans. of NAMRI/SME*, **28**(2000), 131-136.
[33] H.S. CARSLAW, J.C. JAEGER: Conduction of heat in solids, Oxford University Press, 1980.
[34] W. GRZESIK, P. NIESLONY, M. BARTOSZUK: Finite difference analysis of the thermal behaviour of coated tools in orthogonal cutting of steels. *J. Mach. Tools Manuf.,* **44**(2004), 1451-1462.
[35] W. GRZESIK, P. NIESLONY, M. BARTOSZUK: Finite difference method-based simulation of temperature fields for application to orthogonal cutting with coated tools. *Machining Science and Technology*, **9**(2005)4, 529-546.
[36] W. GRZESIK, M. BARTOSZUK: Prediction of temperature distribution in the cutting zone using finite difference approach. 10th CIRP Int. Workshop on Modeling of Machine Operations, Calabria 2007.
[37] H.T. YOUNG, T.L. CHOU: Modelling of tool-chip interface temperature distribution in metal cutting. *J. Mech. Sci*., **36**(1994)10, 931-943.

Received in February 2009